Cross-Flow Flat-Plate Heat Exchanger Using Computational Fluid Dynamics Simulation on Wood Drying Chamber

La Ode Mohammad Firman[1], AbethNovria Sonjaya[2], Budhi M Suyitno[3], Arif Riyadi Tatak[4]

Center of Excellence in New and Renewable Energy
Magister of Mechanical Engineering Program, Faculty of Engineering[1,2,3,4]
Pancasila University, Jakarta, Indonesia

ABSTRACT

Engineered wood must undergo a long period of drying process before it is ready to be used. Therefore, a new heat exchanger technology must be invented to dry the engineered wood more effectively. The quality of the engineered wood is one of the factors influencing the production process. This research was conducted to identify the optimal temperature for drying engineered wood using a cross-flow flat-plate heat exchanger with unmixed fluid arrangement and to determine the heat exchanger's most efficient number of passes.

This research was conducted using the numerical method (CFD simulation) and the Ansys Fluent software. In this research, the viscosity, density, and pressure constant were determined to be at 1 atm. We used air as fluid medium with a mass density of 1,228 kg/m^3, air thermal conductivity of 0.0286 W/m.K, fluid viscosity of $2,0349.10^{-5}$ $N.s/m^2$, steam mass density of 0.689 kg/m^3, and thermal conductivity of 0.0370 W/m.K.

Results showed that, in order to increase the air temperature in the drying chamber, heat energy of 69566.01 kJ/s must flow into the flat-plate heat exchanger. Further calculations show that the heat exchanger's effectiveness (ϵ) was 25% and that the average temperature in the heat exchanger on the air side and the gas side was 68.63 ℃ and 172.5 ℃, respectively.

Keywords: Heat exchanger effectiveness, flat-plate heat exchanger, CFD simulation

1. INTRODUCTION

1.1 Background

The process of analyzing and testing a heat exchanger installed in an engineered wood dryer involves heat transfer mechanisms which take place in a wood drying chamber. Therefore, a heat transfer analysis must be carried out before designing the device. Such analysis must take into account several important aspects: the heat transfer process, physical dimension, and the number of inlet and outlet nozzles in the heat exchanger [1][2][3][4][5].

A laboratory study is required to further identify any changes in air temperature, rate of heat transfer, and the effectiveness of heat exchanger installed in an engineered wood dryer chamber. Engineered wood with a certain level of moisture is placed in a drying chamber to be dried using the heat generated from a cross-flow flat-plate heat exchanger. The temperature is then set within a particular range (60–80 °C) in order to evaporate the moisture [6].

There are some reasons why the cross-flow flat-plate heat exchanger is better than its tubular version (double pipe heat exchanger) [6][7] such as the fact that (1) a flat-plate heat exchanger can save energy up to five times more than the tubular design; (2) its installation requires a smaller space; (3) it is easier to maintain [9]; (4) its capacity is easy to adjust; (5) it decreases operation cost; (6) the average heat transfer and the heat transfer coefficient from nanofluid of both heat exchanger devices are higher than its fluid form (water inflow and outflow); and (7) its efficiency is higher than a tubular (concentric tube) heat exchanger [10].

1.2 Research Objective

This research was conducted to identify the optimal temperature for drying engineered wood using a cross-flow flat-plate heat exchanger with unmixed fluid arrangement and to determine the heat exchanger's most efficient number of passes.

1.3 Methods

Research Location

The research was carried out in 2020 at the Faculty of Engineering's Laboratory, Pancasila University, Jakarta.

Data Collection Method

Data were collected using two methods: literature review and experiments involving a cross-flow flat-plate heat exchanger. The experiments resulted in a set of specification data related to the application of the device.

Data Analysis

Those data were then recorded within a specific timeframe and analyzed using several formulae relevant to each type of data. The calculation results were then simulated using the CFD (Ansys Fluent) software.

Dimension of a Flat-Plate Heat Exchanger on Wood Drying Chamber

Our experiments used several parameters relevant to a flat-plate heat exchanger, namely (1)air mass flow rate of $\dot{m}_a$ = 0.75 kg/s; (2) gas mass flow rate of $\dot{m}_g$ = 0,6 kg/s [11]; (3) inlet air temperature of $T_{a\text{-}in}$ = 30 ºC; and (4) inlet gas temperature of $T_{g\text{-}in}$ = 220 ºC.
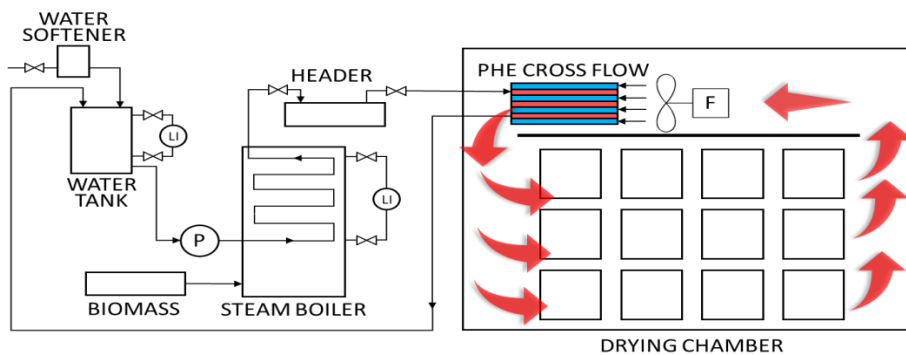

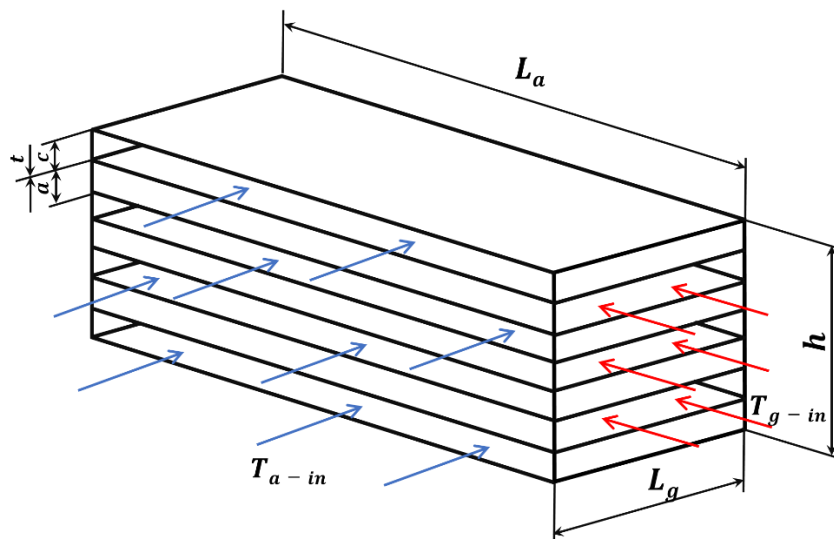Figure 1a.Wood Drying Chamber by using Hot Fluid from Steam Boiler

Figure 1b. Dimension of a Cross-flow Flat-Plate Heat Exchanger

2. RESULT AND DISCUSSION
2.1 Calculation Analysis

The length of the air duct was L_a = 13,800 mm. The width of the heat exchanger was L_g = 800 mm. The thickness of the plate was 0.762 mm. The number of air passes was n_a = 15. The number of gas passes was n_g = 14. The width of each air pass was c = 65 mm. The width of each gas pass was a = 21 mm. The air mass flow rate was $\dot{m}_a$ = 0.75 kg/s. The gas mass flow rate was $\dot{m}_g$ = 0.6 kg/s. The heat energy entering the flat-plate heat exchanger was 69,566.01 kJ/s.

The wet circumference on the air side was P_a= $2L_a$+ $2c$ = 2×13,800 mm+2×65 mm = 27,730 mm.

The wet circumference on the gas side was P_g = $2L_g$+ $2a$ = 2×800 mm+2×21 mm = 1,642 mm.

The sizes of air pass cross section (per pass) were A_{air} = 65 mm×13,800 mm = 897,000 mm^2 = 0.897 m^2 and $A_{air\text{-}total}$ = 0.897×15 = 13.455 m^2.

The sizes of gas pass cross section (per pass) were A_{gas} = 21 mm×800 mm = 16,800 mm^2 = 0.0168 m^2 and $A_{gas\text{-}total}$ = 0.0168×14 = 0.2352 m^2.

The diameter of air duct hydraulics was $D_{H\text{-}air}$ = (4×A_{air})/P_a = (4×897,000 mm^2)/27,730 mm = 129.391 mm = 0.129391 m.

The diameter of gas duct hydraulics was $D_{H\text{-}gas}$ = (4×A_{gas})/P_g = (4×16,800 mm^2)/1,642 mm = 40.926 mm = 0.40926 m.

The total area of heat transfer surface was A_{total} = 2×13,800 mm×800 mm×14 = 397,440,000 mm^2 = 397.44 m^2.

The mass flow rate per air cross-sectional unit area was m_a/A_{air} = 0.75/0.897 = 0.06 kg/s.m^2 and m_g/A_{gas} = 0.6/0.0168 = 2.55 kg/s.m^2.

The temperature of both fluids might vary along the duct. Thus, it was deemed necessary to predict the average temperature and refine our calculation after the outlet temperature had been found [11].

The most satisfactory average cool air temperature was determined to be at 70 ºC (343 K), and, according to the dry air temperature table, we obtained these results: μ_a = 2.0349.10^{-5} N.s/m^2; $P_{r\text{-}a}$= 0.71; k_a = 0.0286 W/kg.K; and $c_{p\text{-}a}$ = 1,018 J/kg.K.

Besides that, we also determined the average hot gas temperature of 200 ºC (473 K). Based on the outlet air temperature leaving the cross-flow flat-plate heat exchanger, we obtained these results: μ_g = 2.5693.10^{-5} N.s/m^2; $P_{r\text{-}g}$ = 0.71; k_g = 0.0370 W/kg.K; and $c_{p\text{-}g}$= 1035 J/kg.K.

Next, we calculated the Reynold number as follows [11].

$$R_{e-air} = \frac{\left(\frac{\dot{m}}{A}\right)_a \times D_{H-air}}{\mu_{a(70°C)}} = \frac{0.06 \frac{\text{kg}}{\text{m}^2 \cdot \text{s}} \times 0.129391 \text{ m}}{2.0349 \times 10^{-5} \text{ kg/m.s}} = 354.4$$

$$R_{e-air} = \frac{\left(\frac{\dot{m}}{A}\right)_g \times D_{H-gas}}{\mu_{g(200°C)}} = \frac{2.55 \frac{\text{kg}}{\text{m}^2 \cdot \text{s}} \times 0.40926 \text{ m}}{2.5693 \times 10^{-5} \text{ kg/m.s}} = 4,063.5$$

Next, we calculated the average unit conductance of each fluid [11]. Given the value of L/D > 20, the air correction factor was calculated as follows.

$$\frac{\bar{h}_{cL}}{\bar{h}_c} = 1 + 6\frac{D}{L} = 1 + 6 \times \frac{129.391 \text{ mm}}{13,800 \text{ mm}} = 1.0563$$

Given the value of L/D < 20, the gas correction factor was calculated as follows.

$$\frac{\bar{h}_{cL}}{\bar{h}_c} = 1 + \left(\frac{D}{L}\right)^{0.7} = 1 + \left(\frac{40.926\text{mm}}{800\text{mm}}\right)^{0,7} = 1.1248$$

If the average unit conductance of air fluid was $\frac{L_a}{D_{H-air}} = 106.65 > 20$, then

$$\bar{h}_{air} = \left[(0.023)\left(\frac{k_{air}}{D_{H-air}}\right)(Re_{air}^{0.8})(Pr_{air}^{0.33})\right]\left[1 + 6\left(\frac{D_{H-air}}{L_{air}}\right)\right]$$
$$= \left[(0.023)\left(\frac{0.0286\text{ W/kg. K}}{0.129391\text{ m}}\right)(354.4^{0.8})(0.71^{0.33})\right] \times \left[1 + 6\left(\frac{0.129391\text{l}}{13,800\text{m}}\right)\right.$$
$$\bar{h}_{air} = 0.66\frac{\text{W}}{\text{m}^2 \cdot \text{K}}$$

If the average unit conductance of air fluid was $L_a/D_{H-gas} = 19.55 < 20$, then

$$\bar{h}_{gas} = \left[(0.023)\left(\frac{k_{gas}}{D_{H-gas}}\right)(Re_{gas}^{0.8})(Pr_{gas}^{0.33})\right]\left[1 + \left(\frac{D_{H-gas}}{L_{gas}}\right)^{0.7}\right]$$
$$= \left[(0.023)\left(\frac{0.0370\text{ W/kg. K}}{0.104673\text{ m}}\right)(4063.5^{0.8})(0.71^{0.33})\right] \times \left[1 + \left(\frac{0.104673\text{m}}{0.800\text{m}}\right)\right]$$
$$\bar{h}_{gas} = 15.73\frac{\text{W}}{\text{m}^2 \cdot \text{K}}$$

If the thermal resistance of the metal wall is ignored, then the overall conductivity was calculated as follows.

$$UA = \frac{1}{\frac{1}{\bar{h}_{air}A_{total}} + \frac{1}{\bar{h}_{gas}A_{total}}}$$
$$UA = \frac{1}{\frac{1}{0.66\frac{\text{W}}{\text{m}^2\cdot\text{K}}\times 397.44\text{ m}^2} + \frac{1}{15.73\frac{\text{W}}{\text{m}^2\cdot\text{K}}\times 397.44\text{ m}^2}} = 253.08\frac{\text{W}}{\text{K}}$$

The number of transfer unit (NTU) was based on the hotter fluid, so the heat conductivity rate was calculated as follows.

$$NTU = \frac{UA}{C_{min}} = \frac{UA}{\dot{m}_{gas} \times c_{p-gas}} = \frac{253.08\text{ W/K}}{0.60\text{ kg/s} \times 1,035\text{ J/kg. K}} = 0.41$$

The comparison between heat capacities per hour was calculated as follows.

$$\frac{C_{gas}}{C_{air}} = \frac{\dot{m}_{gas} \times c_{p-gas}}{\dot{m}_{air} \times c_{p-air}} = \frac{0.60\text{ kg/s} \times 1,035\text{ J/kg. K}}{0.75\text{ kg/s} \times 1,018\text{ J/kg. K}} = 0.81$$

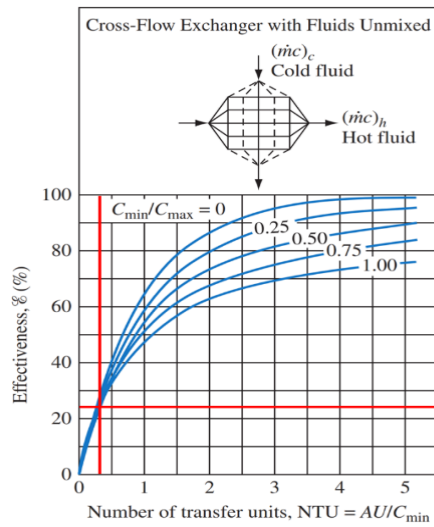The above calculation process resulted in this following effectiveness diagram.

Figure 2. Effectiveness of Cross-flow Heat Exchanger with Unmixed Air and Gas Fluids
(Source: W. M. Kays and A. L., London, Compact Heat Exchangers, National Press, 1955)

Based on the result of our calculation and observation as seen in Figure 2 above, the heat exchanger's effectiveness was determined to be (ϵ) = 25% or 0.25.

The value of air temperature leaving the heat exchanger was [11]

$T_{a\text{-}out} = T_{a\text{-}in} + \{(C_g/C_a) \times \text{\C} \times \Delta T_{max}\}$ = 30 °C + {0.81×0.25×(220 – 30)} °C or $T_{a\text{-}out}$ = 68.63 °C;

The value of gas temperature leaving the heat exchanger was

$T_{g\text{-}out} = T_{g\text{-}in} - \{(\dot{m}_a \times c_{p\text{-}a} \times \Delta T_a)/(\dot{m}_a \times c_{p\text{-}g})\}$ = 220 °C – 47.5 °C = 172.5 °C.

The outlet temperature from the heat exchanger to the wood drying chamber was 68.63 °C, which was relatively close to the assumed value of 172.5 °C, so a second approach was not needed. This research examined the effectiveness of a flat-plate heat exchanger as an eco-friendly device to transfer heat into a wood drying machine based on the total number of tube rows in the shell and tube heat exchanger. After conducting several analyses and tests, we found that a flat-plate heat exchanger could effectively transfer heat into a drying chamber, thus increasing the chamber's temperature by 68.63 °C.

The dimension of the cross-flow flat-plate heat exchanger was 13,800 mm in length and 800 mm in width; it also consisted of a number of aluminum plates, each of which was 0.762 mm in thickness. Aluminum plates are excellent heat conductors which are relatively durable and capable of preserving heat [11]. The device's dimension and inlet and outlet ducts can be adjusted to the user's needs. 14 outlet passes were needed to transfer heated gas resulting from burnt wood waste in order to heat the boiler. Meanwhile, the air which entered and left the device had to undergo 15 passes. In order to generate a 68.63 °C temperature in the wood drying chamber, the outlet temperature of the device had to be 172.5 °C with a 25% effectiveness rate.

2.2 Computational Fluid Dynamics (CFD) Simulation

Computational Fluid Dynamics (CFD) is a method for calculating and predicting fluid flows, heat transfers, and other phenomena, which is carried out numerically using a computer. Generally speaking, CFD analysis involves the finite volume method, which is a numerical technique which transforms partial differential equations representing conservation laws in a differential volume into algebraic discrete equations in a certain volume (element or cell) [12].
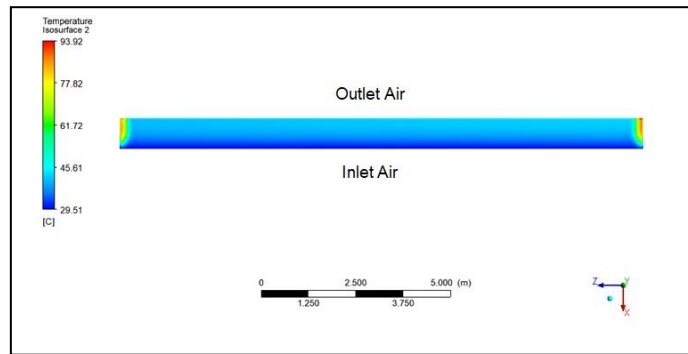
Figure 3. Temperature Contour in Transverse Planes of a Flat-Plate Heat Exchanger in the Air Domain

Figure 3 shows a temperature contour in the form of color gradation which represents different levels of fluid temperature, specifically that of the air fluid which underwent a temperature rise. The color blue at the entrance point represents the moment when the fluid entered at room temperature, whereas the color green at the exit point demonstrates a temperature rise due to the heat transfer from gas fluid in the device.

The temperature of dry air fluid rose as it flowed from the inlet to the outlet ducts, while both ends experienced the highest temperature rise, represented by the color red, because the fluid flow rate on the duct walls was very low. Consequently, the air fluid could receive maximum heat from the gas fluid.
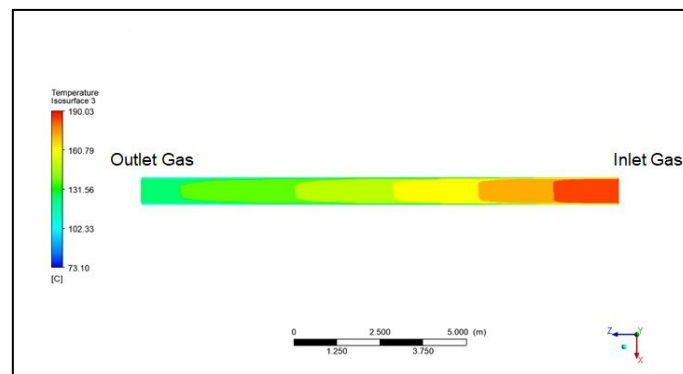

Figure 4. Temperature Contour in Transverse Planes of a Flat-Plate Heat Exchanger in the Gas (Steam) Domain

The above temperature contour resulted from the application of a cross-flow flat-plate heat exchanger in which the fluids were not mixed in the air domain. This result is presented in four frames. Figure 4 shows the color gradation of gas fluid from the inlet to the outlet point. At the inlet point, the fluid generated the color red, which shows a high temperature of 190 ºC, which gradually dropped to 130 ºC as it flowed to the outlet point, shown by the color green. This progression from high to low temperature was due to heat transfer from the gas (steam) fluid to the dry air fluid. In other words, the gas fluid released heat due to the cooler temperature of the dry air fluid.
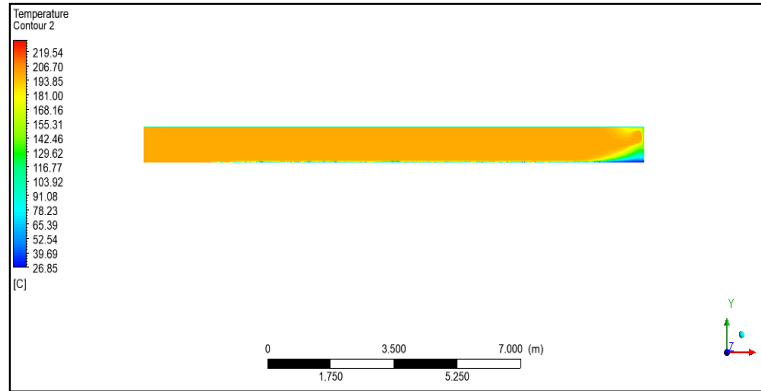
Figure 5.Temperature Contour in Transverse Planes of a Flat-Plate Heat Exchanger (Frame-1)

Figure 5 shows the Frame-1 temperature contour in transverse planes of a flat-plate heat exchanger. This represents the initial condition when the device had not received any air fluid flow along its air duct. The color blue represents the lowest possible air temperature, while the color orange shows the initial condition of the air pass, namely its initial temperature.
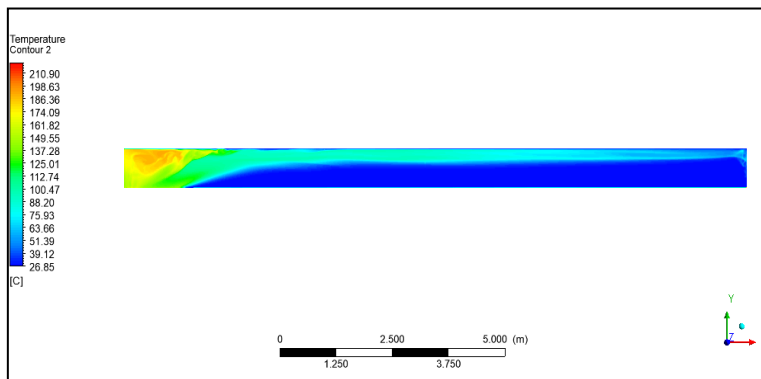

Figure 6.Temperature Contour in Transverse Planes of a Flat-Plate Heat Exchanger (Frame-2)

Figure 6 shows the second frame when the air fluid pass had received heat from the gas (steam) flow beneath the air pass. The color blue represents the lowest possible air temperature, while the color orange shows the point at which the cool air temperature had received heat from the gas or steam. Hotter airflow was identified near the outlet point because the highest heat absorption took place near the exit.

Figure 7.Temperature Contour in Transverse Planes of a Flat-Plate Heat Exchanger
(Frame-3)

Figure 7 shows the third frame when the fluid pass had received heat from the gas or steam flow beneath the air pass. In this graph, the color blue represents the lowest possible air temperature, while the color green shows that the cold air had received heat from the gas or steam. Hotter airflow was identified near the outlet point because the h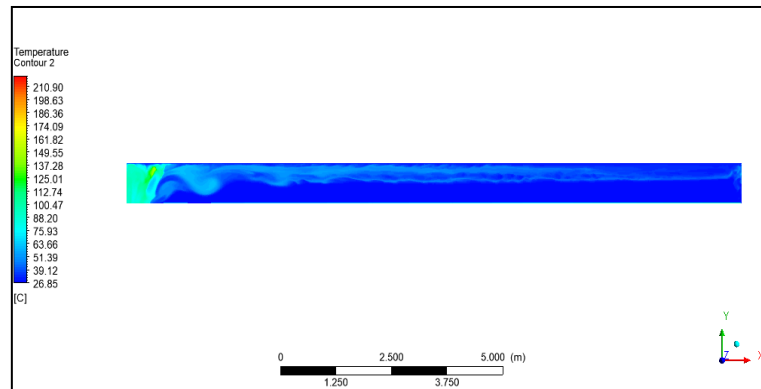ighest heat absorption took place near the exit. The flow took the form of a vortex due to the effect of fluid heating at the gas phase and the effect of viscous fluid flow in the k-epsilon flow model, where the fluid flow at the gas phase affected the temperature distribution of air.
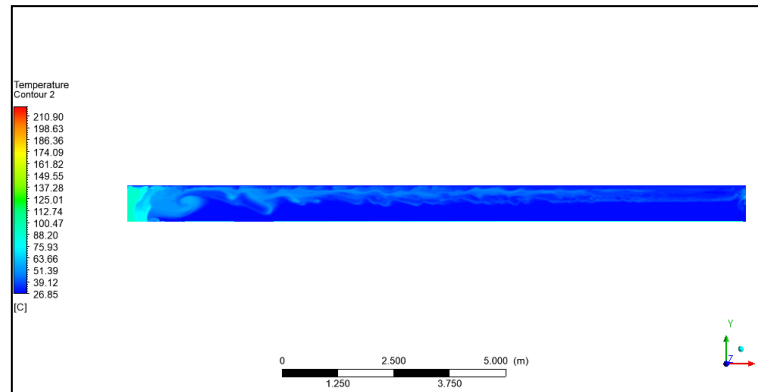

Figure 8.Temperature Contour in Transverse Planes of a Flat-Plate Heat Exchanger
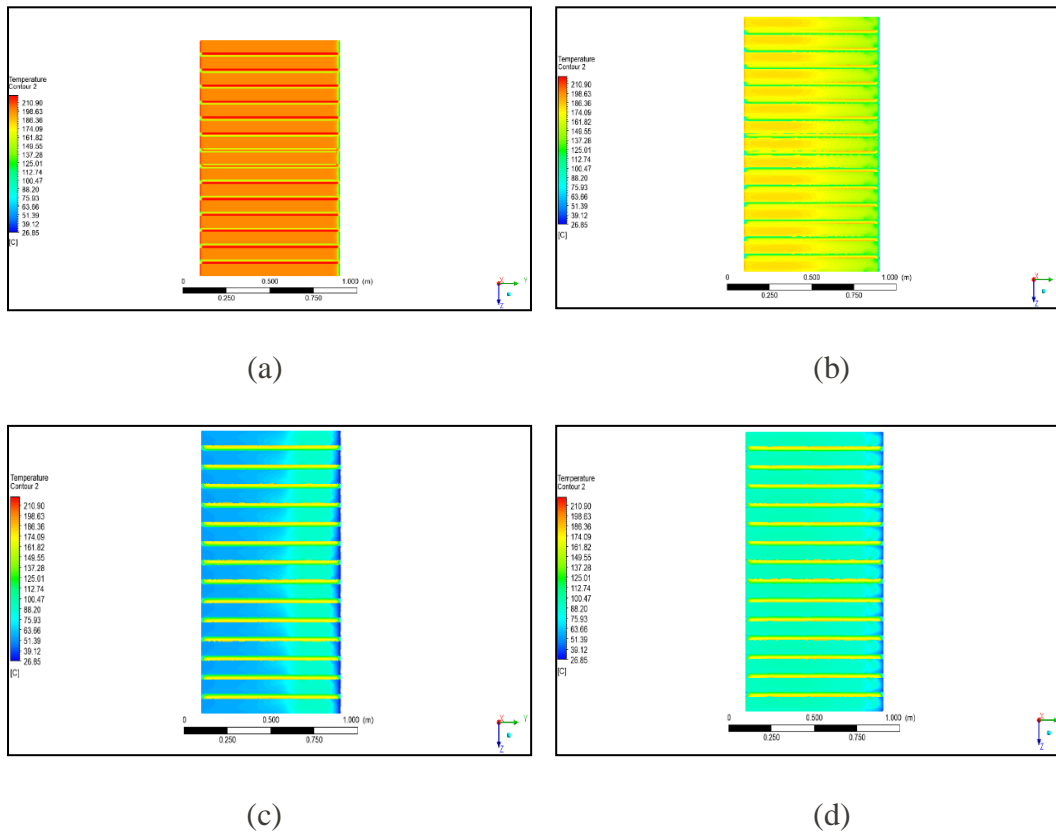(Frame-4)

Figure 8 shows the final frame of air fluid pass in transverse planes. The air fluid underwent heating on the side area of the duct because it absorbed heat from the hot steam with a mass airflow rate of 0.6 kg/s, while the cool air fluid pass had a mass airflow rate of 0.75 kg/s.

The device's temperature contour is also presented in four frontal planes, consisting of (a) Frame-1 frontal plane, (b) Frame-2 frontal plane, (3) Frame-3 frontal plane, and (4) Frame-4 frontal plane. These can be seen in Figure 9.

Figure 9(a) shows the initial condition when the air and gas (steam) fluid passes had not interacted with one another. In the cross-sectional area of the device, there were two types of fluid passes: dry air fluid (shown in orange) and gas or steam fluid (shown in red). Figure 9(a) shows the frontal cross-sectional part of the gas (steam) pass outlet. Figure 9(b) shows the condition where heat transfer took place from the gas to the air fluid. This cross-sectional view shows that the air temperature began to rise from 60 $^{\circ}$C to 180 $^{\circ}$C, where the color green gradually changed into orange. The temperature kept rising as the dry air fluid was flowing towards the outlet. This cross-sectional view is part of the frontal plane of the outlet position of the gas (steam) pass. It can also be seen that at this point the heat transfer had not reached its stable stage.

Figure 9(c) is the third frame which shows the point when the air fluid experienced heat absorption, namely heat transfer from the high-temperature gas (steam) fluid to the low-temperature air fluid. This particular cross-sectional view of the device shows that the inlet area experienced a temperature rise due to the heat from the gas (steam) fluid. Figure 9(d) or the final frame shows the condition when the air fluid had eventually reached its stable stage in terms of heat absorption from the gas (steam) fluid. This cross-sectional view shows that the dry air pass experienced a gradual temperature change as it flowed from the device's inlet to outlet sides, represented by the color blue and yellow, respectively. The green color was

relatively stable at 60 $^{\circ}$C until the fluid reached the outlet side. Meanwhile, the yellowish red color represents the hot gas (steam) pass which transferred its heat to the air fluid.

(a)

(b)

(c)

(d)

Figure 9. Temperature Contour of a Heat Exchanger:
(a) the Frontal Plane (Frame-1), (b) the Frontal Plane (Frame-2),
(c) the Frontal Plane (Frame-3), and (d) the Frontal Plane (Frame-4)

3. CONCLUSION

According to the results of our calculation and CFD simulation on a cross-flow flat-plate heat exchanger, we can draw several main conclusions which are as follows.

1. The cross-flow flat-plate heat exchanger with unmixed air and gas fluids that we used in this research had the following dimension: 13,800 mm in length, 800 mm in width, 65 mm in height for the air pass, and 21 mm in height for the gas pass. Furthermore, it also had 15 air passes and 14 gas passes.

2. The device's effectiveness (ϵ) was found to be 0.25 or 25% because the area where heat transfer could occur was too small for the device to make the best use of the potential heat energy in an efficient way. The relative benefit of heat transfer performance could be achieved by increasing the heat transfer area, while it could be effectively presented in the form of an effectiveness curve.

3. In order to increase the air temperature in the wood drying chamber, the flat-plate heat exchanger required an inflow of 69,566.01 kJ/s of heat energy, while the average temperature of the device's air side and gas side had to be 68.63 $^{\circ}$C and 172.5 $^{\circ}$C, respectively.

REFERENCES

[1] I. G. L. La Ode Mohammad Firman, "Alat penukar kalor untuk mesin pengering RDF," *Teknobiz*, vol. 9, no. 3, pp. 14–19, 2019.

[2] E. Basri and A. Supriadi, "Uji coba mesin pengering kayu kombinasi tenaga surya dan panas dari tungku tipe I," *J. Penelit. Has. Hutan*, vol. 24, no. 5, pp. 437–448, 2006, doi: 10.20886/jphh.2006.24.5.437-448.

[3] Singh, S. K., & Kumar, A. (2020). Experimental study of heat transfer enhancement from dimpled twisted tape in double pipe heat exchanger. Int. J. Mech. Prod. Eng. Res. Dev., 10, 469-482.

[4] Kumar, V. A., & Sathishkumar, N. (2018). Effect of fin geometry for various tubes shape using CFD simulation on multi-channel heat exchanger in mobile air conditioning (MAC). International Journal of Mechanical and Production Engineering Research and Development (IJMPERD) 8 (2018), 2632.

[5] Palanisamy, K., & Nithyanandam, T. (2018). Experimental investigation on convective heat transfer and pressure drop in vertical and horizontal helically coiled tube heat exchanger using MWCNT/water nanofluid. Int J Mech Prod Eng Res Dev, 8, 649-658.

[6] M. Silaban, *Pemanfaatan Termal Surya pada Proses Pengeringan Kayu*, pp. 1–8, 2013.

[7] J. P. Holman, *Heat Transfer, 10th ed*. The McGraw-Hill Companies, Inc., 2010.

[8] La Ode Mohammad Firman, E. Maulana, A. Suwandi, D. Rahmalina, and B. M. Suyitno, "Analysis and testing of heat exchanger for an environmentally friendly RDF drying machine," *Int. J. Mech. Prod. Eng. Res. Dev.*, vol. 10, no. 3, pp. 445–456, 2020, doi: 10.24247/ijmperdjun202041.

[9] K. Slamet, Darmono and E. Lies, "Oven pengering kayu untuk produk mainan kayu ekspor," *J. Ris. Drh.*, pp. 12–20, 2013.

[10] W. D. Daniël Walraven, Ben Laenen, and William D'haeseleer, "Comparison of shell-and-tube with plate heat exchangers for the use in low-temperature organic Rankine cycles," *Energy Convers. Manag.*, vol. 87, pp. 227–237, 2014, doi: 10.1016/j.enconman.2014.07.019.

[11] "5 Reasons to use plate-and-frame heat exchangers instead of shell-and-tube," *www.alfalaval.com*, 2004. [Online]. Available: https://www.alfalaval.com/microsites/gphe/tools/gphe-vs-shell-and-tube/#:~:text=Plate heat exchangers are up,tubes for compact heat exchangers. [Accessed: 14-Feb-2021].

[12] Silaipillayarputhur, K., & KHURSHID, H. (2019). The design of shell and tube heat exchangers–A review. International Journal of Mechanical and Production Engineering Research and Development, 9(1), 87-102.

[13] Thakur, G. A. U. R. A. V., & Singh, G. U. R. P. R. E. E. T. (2017). Experimental invistigation of heat transfer characteristics in Al2O3-water based nanofluids operated shell and tube heat exchanger with air bubble injection. International Journal of Mechanical and Production, 7, 263-273.

[14] Prathyusha, B. G. R., JANJANAM, N., & SANDEEP, K. N. R. G. (2018). Numerical Investigation on Shell & Tube Heat Exchanger with Segmental and Helix Baffles. International Journal of Mechanical and Production Engineering Research and Development, 8 (3), 183-192.

[15] M. Seddiq and M. Maerefat, "Analytical solution for heat transfer problem in a cross-flow plate heat exchanger," *Int. J. Heat Mass Transf.*, vol. 163, p. 120410, 2020, doi: 10.1016/j.ijheatmasstransfer.2020.120410.

[16] M. H. Fard, M. R. Talaie, and S. Nasr, "Numerical and experimental investigation of heat transfer of ZnO/water nanofluid in the concentric tube and plate heat exchangers," *Therm. Sci.*, vol. 15, no. 1, pp. 183–194, 2011, doi: 10.2298/TSCI091103048H.

[17] F. Kreith, *Principles of Heat Transfer, 7th ed.*, vol. 55, no. 5. Cengage Learning, Inc., 2011.

[18] F. Moukalled, L. Mangani, and M. Darwish, *The Finite Volume Method in Computational*

Fluid Dynamics: An Advanced Introduction with OpenFOAM® and Matlab, vol. 113. Springer International Publishing, 2016.